COBEM 2023 27TH INTERNATIONAL CONGRESS OF MECHANICAL ENGENEERING

ABCM Brazilian Society of Mechanical Sciences and Engineering
27th ABCM International Congress of Mechanical Engineering
December 04-08, 2023, Florianópolis-SC, Brazil

COB-2023-0981
EXPERIMENTAL STUDY ON THE ANISOTROPIC BEHAVIOR OF OPEN-HOLE GLASS/POLYESTER AND CARBON/EPOXY COMPOSITE SPECIMENS USING THE DIC TECHNIQUE

Ramon Rudá Brito Medeiros
Letícia Graziele Silva Ribeiro
Federal University of Ceará - UFC, R. Felipe Santiago, N° 411, Cidade Universitária, Russas/CE, CEP 62.900-420.
ramon.ruda@ufc.br; leticia.sribeiro2803@gmail.com

João Pedro Rodrigues Deodato
Rodrigo Nogueira de Codes
Zoroastro Torres Vilar
Federal Rural University of the Semi-Arid Region - UFERSA, R. Francisco Mota, N° 572, Pres. Costa e Silva, Mossoró/ RN, CEP 59.625-900.
jpdeodato@gmail.com; rncodes@ufersa.edu.br; zoroastro@ufersa.edu.br

Kelly Cristiane Gomes
Federal University of Paraíba - UFPB, Campus I, Lot. Cidade Universitaria, João Pessoa/PB, CEP 58.051-900.
gomes@cear.ufpb.br

Abstract. *In most mechanical engineering applications, it is necessary to introduce geometric discontinuities to perform specific functions. The most common example is the hole, which is inserted into structures to allow for unions, attachment of accessories, cable and duct passages, among others. This study investigated the tensile mechanical properties of fiberglass/polyester and carbon fiber/epoxy composites, evaluating the influence of anisotropy under load orientations of 0/90° and ±45°, as well as the behavior of these materials in the presence of a concentric circular hole as a stress concentrator. Strain measurements in the longitudinal and transverse directions on the specimen surface during uniaxial tensile tests were performed using the Digital Image Correlation (DIC) technique, which allowed for measuring the strain distribution profile in the section containing the geometric discontinuity and quantifying the stress concentration caused by it. The mechanical properties obtained in the tests were the ultimate tensile strength, elastic modulus, and fracture strain. The composite laminates exhibited higher stiffness in specimens where the load was applied in the 0/90° orientation. The measured stress concentrations showed different values and are not consistent with the expected values for isotropic materials.*

Keywords: *composite, anisotropy, open-hole, DIC, stress concentration factor.*

1. INTRODUCTION

Composite materials are defined as materials formed by the combination of two or more insoluble materials. This combination or mixture results in a material that exhibits intermediate properties compared to the materials that originated it, allowing the attainment of a material with optimized properties suitable for a specific application (Callister and Rethwisch, 2020).

At least one of the phases present in the composite material will act as the matrix, while the other materials will serve as filler or reinforcement. The matrix is the predominant phase in the composite, and its main function is to bind the other materials together. The reinforcement materials are dispersed within the matrix, playing a crucial role in enhancing (increasing) the mechanical properties of the composite (Daniel and Ishai, 2006).

The utilization of composite materials in the production of components offers several advantages. Among these advantages, it is worth mentioning the production of components with fewer process steps, as well as the production of parts in their final state (Ansar et al., 2011; Warren et al., 2015; Saleh et al., 2016). Another advantage is related to the mass of the produced components, as composite materials enable the manufacturing of relatively lighter structural parts compared to conventional structural materials such as steel and aluminum. This characteristic is due to the low density of composite materials (Mingming et al., 2017; Morais, 2000). These features make composite materials a good choice in structural, military, automotive, sports, and other applications (Ansar et al., 2011; Warren et al., 2015; Saleh et al., 2016).

The most commonly used reinforcement fibers in the production of structural components are glass, carbon, and aramid fibers. However, fiberglass-reinforced plastics are the most common and widely used, mainly due to their low cost (Tinô and Aquino, 2016). Carbon fiber composites are more commonly used in high-performance structural

applications, despite their higher cost compared to fiberglass composites. On the other hand, aramid fiber composites find more focused applications in energy absorption. It is important to note that among these three mentioned composites, the ones made with aramid fibers have the lowest density, followed by carbon fiber composites, and finally, fiberglass composites (Daniel and Ishai, 2006).

The presence of geometric discontinuities, such as holes, is of paramount importance in structures, as various structural applications, including aerospace and automotive, incorporate a significant number of engineered holes. Holes are introduced into structures to enable connections, attachment of accessories, routing of electrical cables, hydraulic ducts, and more (Khashaba and Khdair, 2017; Shafighfard et al., 2019; Yudhanto et al., 2012).

Geometric discontinuities cause significant changes in stress distribution within the cross-section containing them, resulting in stress concentration in the vicinity of these discontinuities (Yudhanto et al., 2012). This can lead to premature failure of the component (Pierron et al., 2007; Koord et al., 2020), especially in polymer composites that exhibit brittle behavior, which directly influences the final fracture of the material (Mollenhauer et al., 2006).

Understanding the stress distribution and stress concentration around notches is crucial to increase the reliability of the design, particularly when the employed material exhibits anisotropic behavior, as is the case with composite materials (Dandekar and Shin, 2012; Mingming et al., 2017; Hallett and Wisnom, 2006).

The need to understand the mechanical behavior of laminated composite materials with geometric discontinuities, especially circular holes, has prompted numerous studies on the fracture mechanics of these materials (Yudhanto et al., 2012; Camanho et al., 2007; Dandekar and Shin, 2012).

Most studies conducted on composites with stress concentrators adopt an experimental and/or numerical approach (Wang et al., 2004; Sun et al., 2020). These studies demonstrate that there are several variables that can influence the results. Among these variables, material properties, manufacturing processes, notch geometry, fiber orientations, stacking sequence, layer thicknesses, among others, can be mentioned (Green et al., 2007; Zhu et al., 2018).

The present paper aims to conduct a comparative study of the mechanical properties of two composite laminates: one reinforced with fiberglass and the other with carbon fiber. The study will analyze the anisotropic effects under load orientations of 0/90° and ±45°, as well as examine the behavior of these two laminates in the presence of a concentric circular hole and quantify the stress concentration caused by this notch.

2. MATERIALS AND METHODS

2.1 Lamination of composites

In the development of the present work, two distinct laminates were manufactured: one laminate composed of a polyester matrix with fiberglass fabric, and another formed by an epoxy matrix and carbon fiber fabric. Both laminates were manufactured with eight layers of fabric, where each fabric layer was oriented in the same direction.

The fiberglass laminate was made with a thermosetting polymer matrix of unsaturated orthophthalic polyester, from the brand Veloflex. The resin's curing agent/catalyst used was methyl-ethyl-ketone peroxide (MEKP) in a ratio of 1% by volume of resin, providing a gel time of 10 to 15 minutes at 25°C. For the structural reinforcement, a bidirectional fabric with a plain weave of E-glass fiber was used, commercially known as RE200P, with a basis weight of 200 ± 20 g/m², warp and weft density of 5 ± 0.2 yarns/cm, and thickness of 0.21 ± 0.3 mm.

The carbon fiber laminate, on the other hand, was obtained using a low-viscosity thermosetting resin, commercially known as LR135 Epoxy Resin. The curing agent used is a commercial product called LH 137 Epoxy Hardener, with a mixing ratio by weight of 100 parts resin to 33 parts hardener (100:33), resulting in a gel time of approximately 60 minutes at 25°C. The carbon fiber fabric used is marketed under the name RC200P, produced from a weave of High Strength 3k carbon fibers, with a basis weight of 197 ± 20 g/m², warp and weft density of 5 ± 0.2 yarns/cm, and thickness of 0.22 ± 0.3 mm.

The composite laminations were carried out on a 10 mm thick glass sheet using a carnauba wax-based mold release agent, commercially known as TR Mold Release. The fabrics were impregnated layer by layer with resin, and a brush and roller were used to remove excess resin. The fiberglass laminate was produced by the hand lay-up process, while the carbon fiber laminate was obtained through the vacuum bag process. Both laminates were produced with a size of 500 x 500 mm and subsequently cut to obtain the necessary samples and test specimens.

2.2 Cutting of specimens and configurations

The samples used in the experimental procedures of this study were cut using a circular saw with a segmented diamond blade, specifically the IRWIN ϕ4.3/8" x 3/4" blade. Subsequently, the samples were sanded and polished to achieve the required finish and dimensional tolerance. For the samples that required circular holes of 6 mm, the holes were made using a milling machine with a high-speed steel (HSS) end mill, with a cutting speed of 40 mm/s (Cunha, 2020). Finally, the test specimens were spray-painted black and sprayed with white droplets, creating a gray pattern texture on the specimen surface, necessary for the use of the Digital Image Correlation (DIC) technique.

The test specimens for uniaxial tensile testing and uniaxial tensile testing with a concentric hole followed the guidelines of ASTM D3039/D3039M (2017) and ASTM D5766/D5766M (2018), respectively. The geometry and dimensions of these test specimens are illustrated in Figure 1. The configurations of the test specimens for the tensile tests, as well as their nomenclature, are presented in Table 1. Three test specimens were produced for each studied configuration. Five samples measuring 25 x 25 mm were used for determining the density of each laminate.

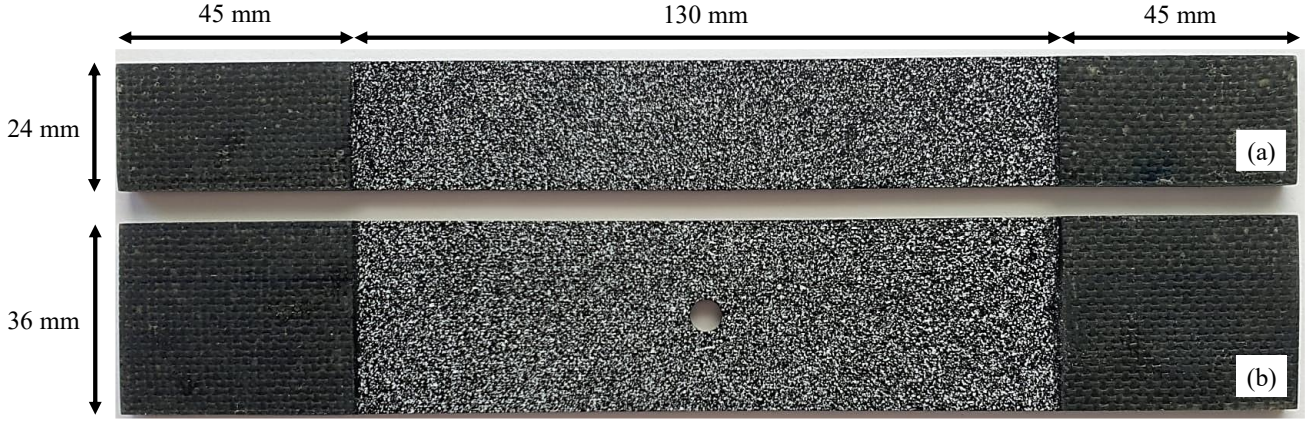

Figure 1. Geometry and dimensions of the test specimens: (a) Specimens ASTM D3039/D3039M (2017); (b) ASTM D5766/D5766M (2018).

Table 1. Test specimen settings.

Laminate	Specimens	Definition
E-glass Fiber Composite (GFC)	T.GFC.0°	Traction test on the GFC: Load applied in the direction of the fiber, fabric in the 0/90° orientation.
	T.GFC.45°	Traction test on the GFC: Load applied at ±45° from the direction of the fiber, fabric in the ±45° orientation.
	TH.GFC.0°	Traction test on the GFC with hole 6 mm: Load applied in the direction of the fiber, fabric in the 0/90° orientation.
	TH.GFC.45°	Traction test on the GFC with hole 6 mm: Load applied at ±45° from the direction of the fiber, fabric in the ±45° orientation.
Carbon Fiber Composite (CFC)	T.CFC.0°	Traction test on the CFC: Load applied in the direction of the fiber, fabric in the 0/90° orientation.
	T.CFC.45°	Traction test on the CFC: Load applied at ±45° from the direction of the fiber, fabric in the ±45° orientation.
	TH.CFC.0°	Traction test on the CFC with hole 6 mm: Load applied in the direction of the fiber, fabric in the 0/90° orientation.
	TH.CFC.45°	Traction test on the CFC with hole 6 mm: Load applied at ±45° from the direction of the fiber, fabric in the ±45° orientation.

2.3 Density test

In accordance with the guidelines of ASTM D792 (2020), using Method A for the characterization of solid plastics in water, five samples of each laminate measuring 25 x 25 mm were used. The masses of the samples were measured on a Marte AD330 digital balance with a maximum capacity of 340 g and a resolution of 0.01 g.

2.4 Uniaxial tensile test

The uniaxial tensile tests followed the guidelines of ASTM D3039/D3039M (2017) and ASTM D5766/D5766M (2018) and were conducted on an EMIC DL10000 universal testing machine, equipped with a 30 kN load cell and a test speed of 0.008 mm/s. The strain measurements of the samples were performed using the Digital Image Correlation (DIC) technique. For this purpose, images during the tensile tests were captured by a CANON D60i digital camera with a 100 mm macro lens. The image acquisition was performed every 5 seconds. Figure 2 illustrates the setup of the experimental apparatus.

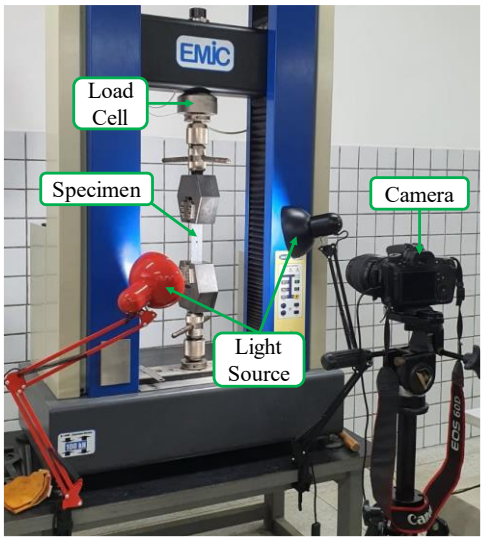

Figure 2. Experimental setup of the tensile test.

The processing of the images obtained during the tests was carried out using the NCORR V1.2 software, which is an open-source 2D digital image correlation program. In addition to being free, NCORR has an accessible and intuitive graphical user interface, and it is fully integrated with the MATLAB® environment (Blaber et al., 2015).

From the tests, it was possible to determine the following mechanical properties of the material: ultimate tensile strength (σ_{ut}), longitudinal elastic modulus (E_y), and fracture strain (ε_{ut}). Additionally, it was possible to determine the strain distribution across the entire surface of the test specimen, providing data to determine the stress concentration caused by the presence of the geometric discontinuity in the specimen.

2.5 Residual properties and stress concentrator

The assessment of strength loss caused by the presence of geometric discontinuities in composite materials can be conducted through the Residual Strength (RS). In a simplified manner, RS allows quantifying the impact caused by the existence of a geometric discontinuity in a composite, which was determined by Eq. (1) (Acmc et al., 2020).

$$RS = \frac{\sigma_N}{\sigma_{ut}} \tag{1}$$

Where σ_N is the average tensile strength of the specimens with geometric discontinuity, considering the cross-sectional area without the discontinuity.

With the use of the DIC technique, it was possible to measure the strain distribution profile along the cross-section of the specimen containing the hole, particularly in the region around the hole's edge. Thus, the stress concentration factor (K_t) caused by the circular hole was determined by Eq. (2) (Fontes, 2017). It is important to note that Eq. (2) is valid only for the linear elastic regime.

$$K_t = \frac{\sigma_{max.}}{\sigma m} = \frac{E_y . \varepsilon_{max.}}{\sigma m} \tag{2}$$

Where $\sigma_{max.}$ is the maximum stress at the hole edge, σm is the average normal stress in the cross-section containing the hole, and $\varepsilon_{max.}$ is the maximum strain at the hole edge.

3. RESULTS AND DISCUSSION

3.1 Density and thickness of laminates

The obtained data for the density of the laminates used in this study are presented in Table 2. Both produced laminates exhibited low density compared to steel and aluminum alloys, being 7.80 g/cm³ and 2.80 g/cm³, respectively (Daniel and Ishai, 2006). The low density is an important and required characteristic in composites for structural applications, and thus, both laminates meet this requirement.

Table 2. Density and thickness of laminates.

Laminate	Density (g/cm³)	Thickness (mm)
E-glass Fiber Composite (GFC)	1.690 ± 0,012	1.85 ± 0.08
Carbon Fiber Composite (CFC)	1.404 ± 0,010	1.91 ± 0.05

The standard deviations of the densities for both laminates showed close values, being 0.710% for the GFC laminate and 0.712% for the CGC laminate. The low standard deviation indicates that the samples of each laminate exhibited similar characteristics, suggesting that the laminates were homogeneous throughout their extent.

Considering the density of E-glass fiber as 2.54 g/cm³ and the polyester matrix as 1.20 g/cm³, and assuming that the amount of voids within the laminate is negligible, it can be stated that the volumetric fractions of matrix and reinforcement in the GFC laminate were approximately 63.4% and 36.6%, respectively. For the CFC laminate, considering the density of carbon fiber as 1.76 g/cm³ and epoxy matrix as 1.11 g/cm³, also neglecting the presence of voids, the volumetric fraction of carbon fiber is 43.3% and the epoxy matrix is 54.70%. The main justification for the higher matrix fraction in the GFC laminate compared to the CFC laminate is the lamination process. In the hand lay-up lamination process, there is no precise control of the matrix quantity, while the vacuum bag process allows for the removal of excess matrix used in the composite lamination.

Regarding the thickness of the laminates, it was found that the GFC laminate has a smaller value compared to the CFC laminate, as well as the thicknesses of the fabrics. The standard deviation of the GFC laminate was 4.32% and for the CFC laminate was 2.62%, a fact justified by the better control of the vacuum bag lamination process.

3.2 Mechanical tensile properties of laminates (unnotched specimens)

From the tensile tests of the unnotched specimens, it was possible to plot the stress-strain curves of the studied configurations (Figure 3). The tensile mechanical properties of the configurations are presented in Table 3.

Figure 3. Stress-strain curve for T.GFC.0°, T.GFC.45°, T.CFC.0°, and T.CFC.45°.

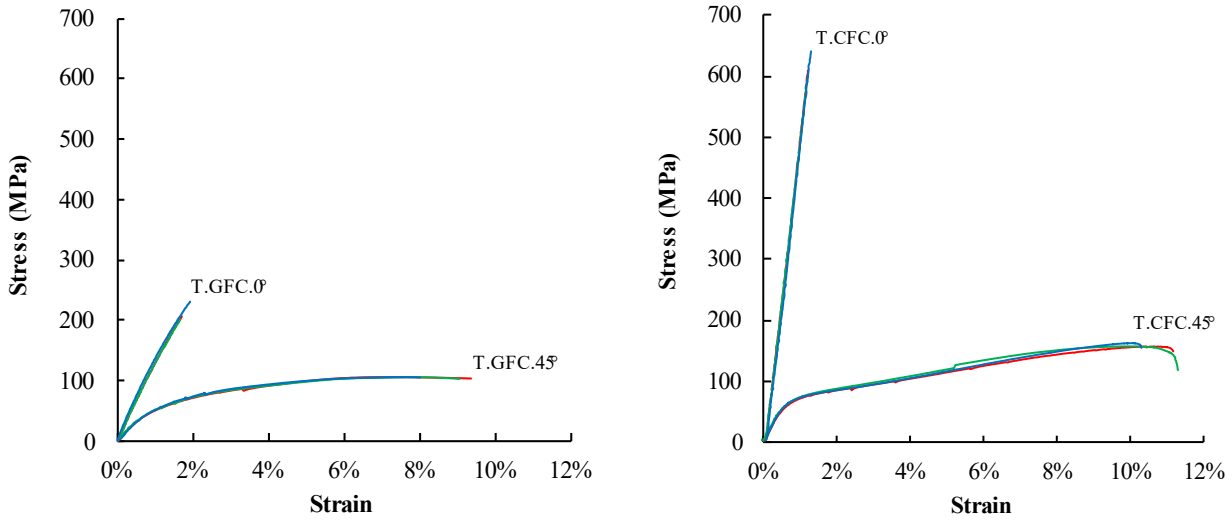

Table 3. Mechanical properties of laminates (unnotched).

Specimens	σ_{ut} (MPa)	E_y (GPa)	ε_{ut} (%)
T.GFC.0°	202.968 ± 3.691	14.339 ± 0.846	1.613 ± 0.157
T.GFC.45°	105.779 ± 0.627	7.024 ± 0,413	8.820 ± 0.710
T.CFC.0°	617.838 ± 21.599	48.772 ± 2.947	1.225 ± 0.058
T.CFC.45°	158.927 ± 3.809	12.193 ± 0.744	10.920 ± 0.565

Based on the data from Table 3, the higher tensile strength of the CFC laminate compared to the GFC laminate was evident. For the average strength values, the T.CFC.0° configuration is approximately 300% stronger than the T.GFC.0° configuration. In the same configuration, the CFC laminate exhibits a stiffness around 3.4 times higher than the GFC laminate. However, in terms of strain at failure, the GFC laminate deforms over 30% more than the CFC laminate. The

higher values observed in the mechanical properties of the CFC laminate are attributed to the carbon fiber reinforcement compared to the fiberglass-reinforced composite.

For the configurations where the load is applied to the specimens with an orientation of ±45° with respect to the reinforcement fibers, the differences between the mechanical properties of the CFC laminate and the GFC laminate are smaller. The tensile strength of T.CFC.45° is 1.5 times higher than that of T.GFC.0°. For these same configurations, the stiffness of CFC is approximately 70% higher, and the strain at failure is about 23% higher.

In terms of laminate anisotropy, the differences in mechanical properties between the T.CFC.45° and T.GFC.45° configurations are smaller compared to the T.CFC.0° and T.GFC.0° configurations. This is due to the load not being applied longitudinally to the fibers, where carbon fibers exhibit significantly higher strength than glass fibers. With the ±45° orientation, the laminates show lower stiffness, with a reduction of nearly 50% in the GFC laminate and 75% in the CFC laminate. Regarding strain at failure, the GFC laminate had an increase of over 400% by simply changing the load orientation, while the CFC laminate showed an increase of over 800%.

Comparing the obtained data with other studies, Fontes (2017) conducted research on fiberglass-reinforced composites using reinforcement fabric with similar characteristics to the present study, but without weft and with a lower grammage. He obtained a tensile strength of 297 MPa for a configuration similar to T.GFC.0° and an average value of 105 MPa for a configuration similar to T.GFC.45°. The difference in the obtained value can be justified by the fact that the non-woven fabric in the T.GFC.0° configuration has the fibers arranged more efficiently to withstand the tensile load that directly acts on them, as they are parallel to the direction of the applied load.

3.3 Tensile tests on specimens with holes (notched specimens)

From the tensile tests of the notched specimens, it was possible to measure the tensile strength of the notched specimens, which allowed determining the residual strength for each laminate configuration, as presented in Table 4.

Table 4. Tensile strength of notched laminate, resistência residual and stress concentration factor.

Specimens	σ_N (MPa)	RS	K_t
TH.GFC.0°	98.147 ± 1.854	0.484 ± 0.013	1.827 ± 0.055
TH.GFC.45°	84.175 ± 4.332	0.796 ± 0.041	1.620 ± 0.066
TH.CFC.0°	299.868 ± 8.980	0.485 ± 0.022	1.644 ± 0.179
TH.CFC.45°	131.927 ± 2.612	0.830 ± 0.026	1.196 ± 0.050

The average values obtained for RS in the TH.GFC.0° and TH.CFC.0° configurations were equal. For the TH.GFC.45° and TH.CFC.45° configurations, although the average values were different, statistically, the results were considered equal, as the standard deviations intersect. In this study, the RS analysis suggests that the damage caused to the laminates by the presence of the notch is determined solely by the geometry since statistically, the data obtained in the studied configurations were similar for both GFC and CFC laminates.

According to Daniel and Ishai (2006), in laminates reinforced with boron fiber fabric in configurations similar to TH.CFC.45°, RS values ranging from 0.833 to 0.909 were obtained. This supports the suggestion that RS is strongly influenced by geometry rather than the composite's reinforcement fiber.

The data obtained for the TH.GFC.45° configuration were almost identical to those obtained by Fontes (2017), who obtained an RS value of 0.773 in laminates reinforced with fiberglass with a similar composition and configuration as TH.GFC.45°.

3.4 Stress concentration and strain distribution in the notched specimens

To determine the stress concentration caused by the hole, longitudinal strains along the cross-section containing the hole were plotted (Figure 4 and Figure 5). Stress magnitudes around 30% of σ_N were selected, ensuring that the test specimens were subjected to a condition in the linear elastic region. The values obtained for K_t are presented in Table 4.

Just like in the RS analysis, the TH.GFC.0° and TH.CFC.0° configurations showed statistically the same result for stress concentration, despite the different mean values of K_t obtained. However, for the TH.GFC.45° and TH.CFC.45° configurations, it can be stated that the stress concentration was more intense in the GFC laminate, approximately 35% higher compared to the mean values.

For isotropic materials, the value of K_t is solely a function of the geometry of the test specimen. Considering the geometry with a width of 36 mm and a 6 mm hole, according to Pilkey and Pilkey (2008), the value of K_t is 2.58, and according to Norton (2013), the value is 2.60, which are much higher than the experimental values obtained for the laminates. This highlights the importance of understanding the behavior of composite materials for the proper design of structures in which they are used.

From the strain distribution profiles in Figure 4 and Figure 5, it can be observed that for the TH.GFC.0° and TH.CFC.0° configurations, the strain distribution tends to stabilize or vary little from 4 mm from the side edges of the

holes (-7 and 7 mm on the graph axes). In contrast, for the TH.GFC.45° and TH.CFC.45° configurations, the uniformization of strain begins to occur from 5 mm from the edges. Although the values of K_t are higher in the 0° configurations, in the ±45° configurations, the highest strains occur at a greater distance from the hole edge. This fact was also observed prior to the fracture of the test specimen, where cracks propagated more in the ±45° configurations.

Figure 4. Distribution of strain in the cross-section of test specimens with holes. (a) TH.GFC.0°. (b) TH.GFC.45°.

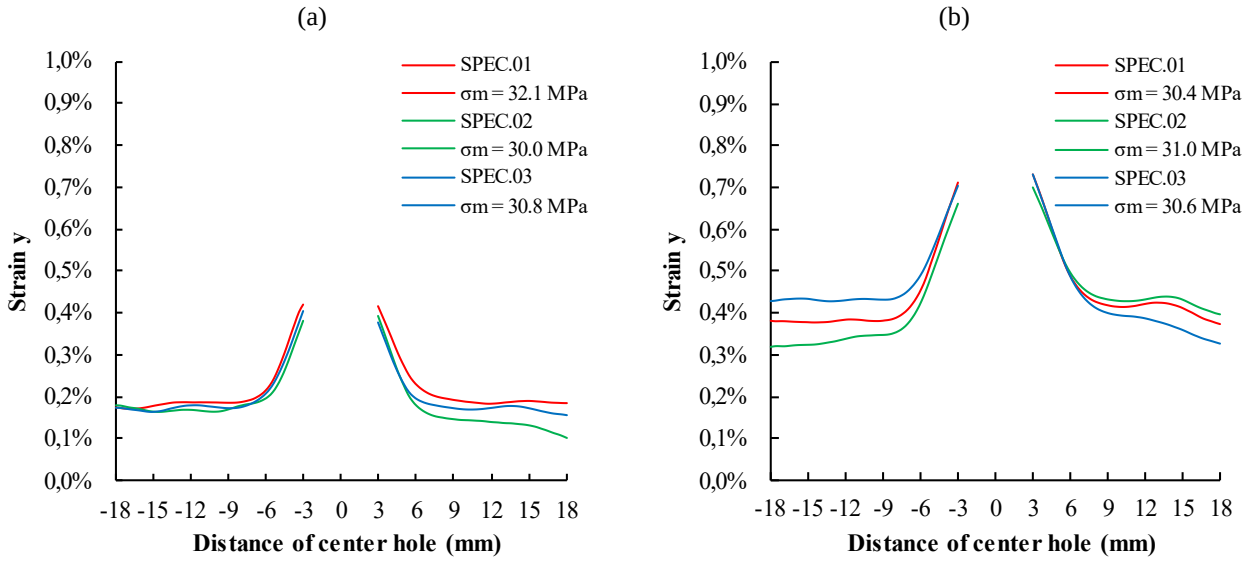

Figure 5. Distribution of strain in the cross-section of test specimens with holes. (a) TH.CFC.0°. (b) TH.CFC.45°.

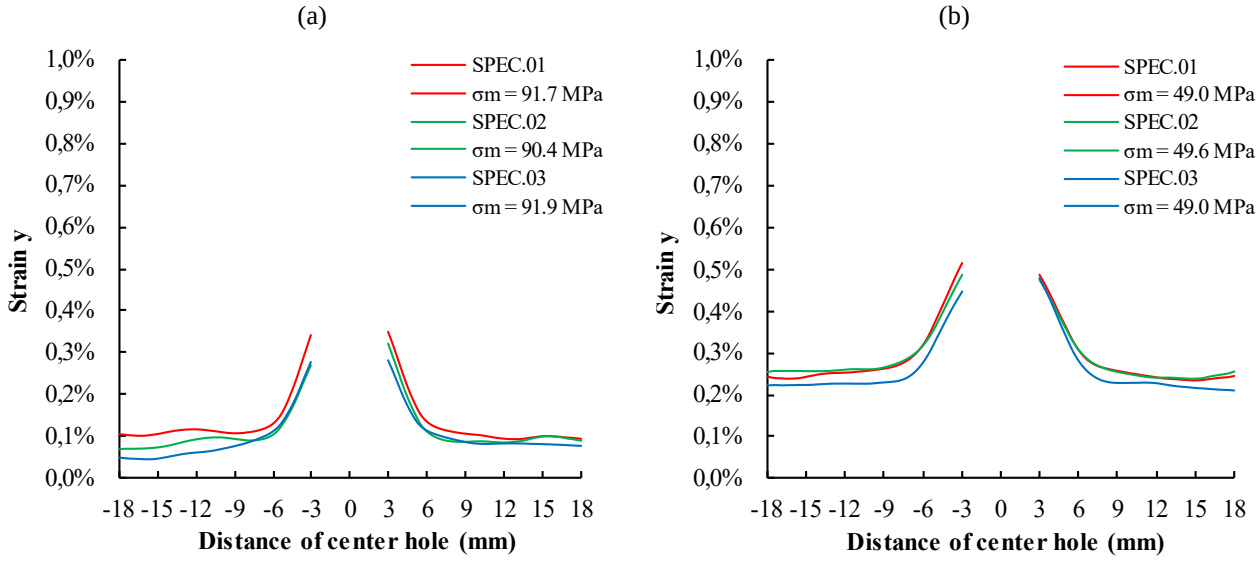

Figure 6 and Figure 7 illustrate the strains on the surface of a test specimen for each studied laminate configuration. The strains are plotted on the x and y axes, corresponding to the horizontal and vertical axes, respectively. The strains were represented for a stress state close to the rupture of the test specimen.

It is evident that the strains along the x-axis for the TH.GFC.0° and TH.CFC.0° configurations vary little in the test specimens of these configurations, due to the high rigidity of the material compared to the other configurations. This high rigidity results in a higher strain peak along the y-axis at the sides of the hole. It can be observed that one side of the hole has a higher strain peak than the other side, due to the material heterogeneity, where the fracture initiates on one side and not instantaneously on both sides of the hole, or due to the fact that the hole is never exactly centered.

The pattern of strains along the y-axis for the TH.GFC.45° and TH.CFC.45° configurations presents a very similar shape, although with distinct magnitudes. In these configurations, which are less rigid, the progression of strain along the test specimen is more visible, as well as the strain peaks on each side of the hole that resemble each other more closely.

Furthermore, in terms of strain along the y-axis, a region in the shape of an "X" in light green shade can be observed, where fracture propagation occurred in the test specimens.

Figure 6. Strain in specimen TH.GFC.0° and TH.GFC.45°.

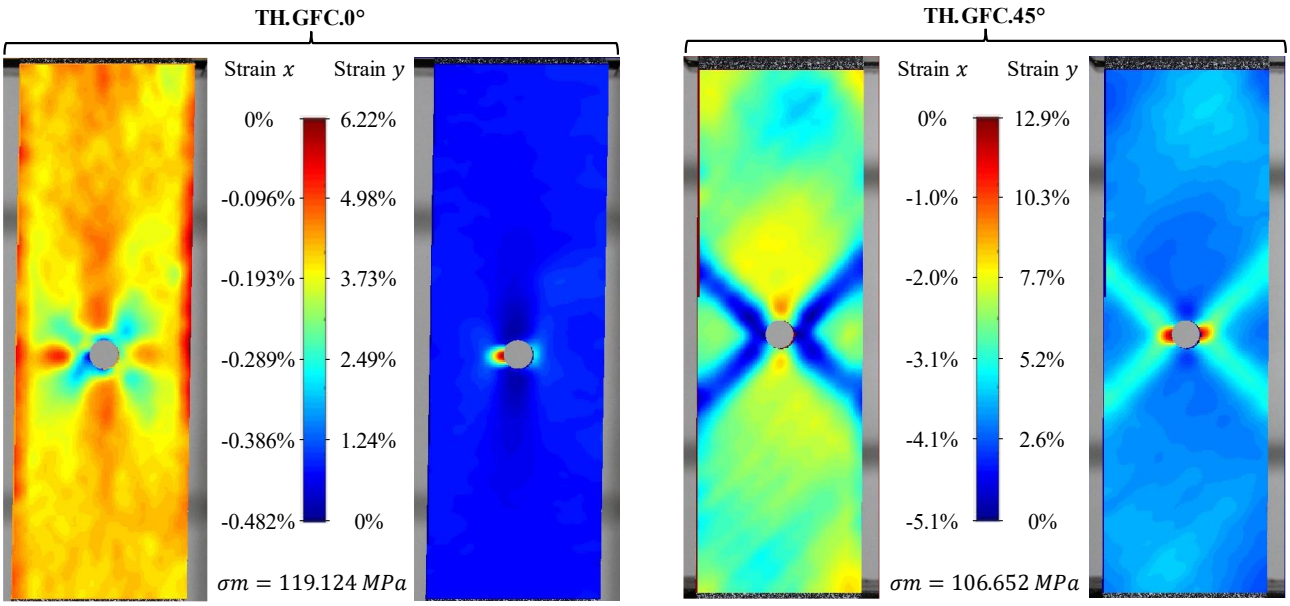

Figure 7. Strain in specimen TH.CFC.0° and TH.CFC.45°.

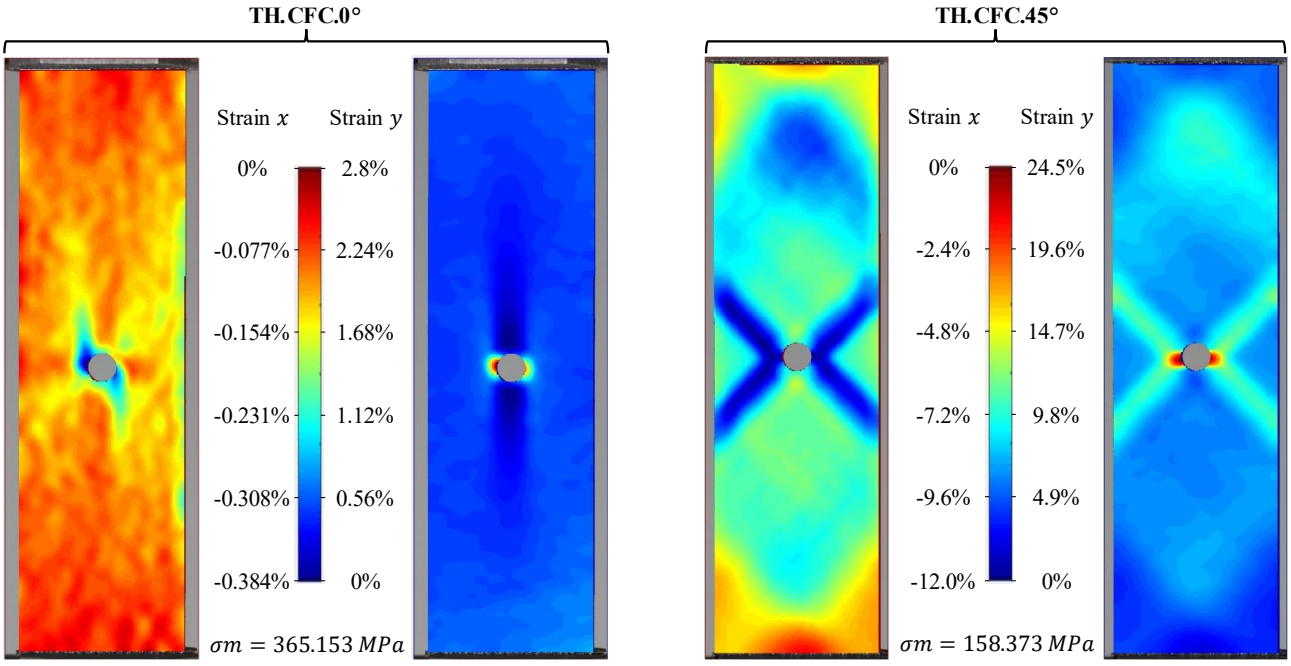

4. CONCLUSIONS

After subjecting the CFC and GFC specimens to tensile testing and analyzing the strain using DIC, it was observed that in both fiber orientations, carbon fiber composites are stronger and stiffer compared to the fiberglass composite specimens. Due to the anisotropic nature of the material, the difference in tensile strength and modulus of elasticity between the T.CFC.0° and T.GFC.0° configurations is twice as large as that between the T.CFC.45° and T.GFC.45° configurations.

Comparing the 0/90º and ±45º configurations, it is observed that in the latter, the strain until failure is significantly higher than in the former. When considering the difference in materials, it is noted that in the T.GFC.0º specimens, the strain is higher compared to the T.CFC.0º specimens, while in the T.GFC.45º and T.CFC.45º specimens, the carbon fiber specimens exhibit greater strain. In the first comparison, this difference can be attributed to the higher ductility of fiberglass compared to carbon fiber, while in the second comparison, the increased strain in both cases is due to the improved interaction between the matrix and the reinforcement, resulting from the anisotropic behavior.

With regards to the behavior in the presence of a concentric circular hole, the damage caused to the material depends solely on the geometry of the notch. The specimens showed equal average values of residual strength for the TH.CFC.0° and TH.GFC.0° configurations, and statistically equal values for the TH.CFC.45° and TH.GFC.45° configurations. The stress concentration caused by the hole is the same for the 0/90° configuration of both matrices, and it is higher in the fiberglass specimens, where the load is applied at ±45°.

With the DIC analysis, it was observed through the strain profile around the hole that in the TH.CFC.0° and TH.GFC.0° configurations, cracks propagate perpendicular to the loading direction. In the TH.CFC.45° and TH.GFC.45° configurations, however, propagation occurs in an X-shaped region.

Finally, unlike traditional methods such as strain gauges that measure strain at specific predetermined points before conducting the test, DIC analyses enable the evaluation of the complete distribution of strain in the test specimen at any defined point after the test. Therefore, they offer advantages over classical methods and are of utmost importance for material characterization, particularly in studies of stress concentration caused by notches.

5. REFERENCES

Acmc, B., Srl, T., Rs, F., Shs, N. and Emf, A., 2020. "Analytical, experimental and finite element analysis of the width/diameter hole ratio effect in vinylester/carbon hybrid twill weave composites". *Composites Part C: Open Access*, Vol. 2, No. 100033, p. 100033.

Ansar, M., Xinwei, W. and Chouwei, Z., 2011. "Modeling strategies of 3D woven composites: A review". *Compos. Struct.*, Vol. 93, No. 8, pp. 1947–1963.

ASTM D3039/D3039 M-17. *Standard test method for tensile properties of polymer matrix composite materials*. Annual Book of ASTM Standards. West Conshohocken, PA: ASTM International, 2017.

ASTM D5766/D5766 M-11. *Standard Test Method for Open-Hole Tensile Strength of Polymer Matrix Composite Laminates*. Annual Book of ASTM Standards. West Conshohocken, PA: ASTM International, 2018.

ASTM D792-20. *Standard test methods for density and specific gravity (relative density) of plastics by displacement*. Annual Book of ASTM Standards. West Conshohocken, PA: ASTM International, 2020.

Blaber, J., Adair, B. and Antoniou, A., 2015. "Ncorr: Open-source 2D digital image correlation matlab software". *Exp. Mech.*, Vol. 55, No. 6, pp. 1105–1122.

Callister, Jr, W.D. and Rethwisch, D.G., 2020. *Callister's Materials Science and Engineering*. John Wiley & Sons, Nashville, TN, 10th edition.

Camanho, P.P., Maimi, P. and Davila, C.G., 2007. "Prediction of size effects in notched laminates using continuum damage mechanics". *Compos. Sci. Technol.*, Vol. 67, No. 13, pp. 2715–2727.

Cunha, R.A.D., 2020. *Comportamento mecanico de um composito intraply/yarn submetido a impacto de baixa velocidade na presenca de concentracao de tensao: uma analise experimental e analitica*. Ph.D. thesis, Graduate Program in Mechanical Engineering, Federal University of Rio Grande do Norte, Natal, Brazil.

Dandekar, C.R. and Shin, Y.C., 2012. "Modeling of machining of composite materials: A review". *Int. J. Mach. Tools Manuf.*, Vol. 57, pp. 102–121.

Daniel, I.M. and Ishai, O., 2006. *Engineering mechanics of composite materials*. Oxford University Press, New York, NY, 2nd edition.

Fontes, R.S., 2017. *Compositos polimericos reforcados por tecidos multiaxiais acoplados: anisotropia, configuracao e concentracao da deformacao*. Ph.D. thesis, Graduate Program in Mechanical Engineering, Federal University of Rio Grande do Norte, Natal, Brazil.

Green, B.G., Wisnom, M.R. and Hallett, S.R., 2007. "An experimental investigation into the tensile strength scaling of notched composites". *Compos. Part A Appl. Sci. Manuf.*, Vol. 38, No. 3, pp. 867–878.

Hallett, S.R. and Wisnom, M.R., 2006. "Experimental investigation of progressive damage and the effect of layup in notched tensile tests". *J. Compos. Mater.*, Vol. 40, No. 2, pp. 119–141.

Khashaba, U.A. and Khdair, A.I., 2017. "Open hole compressive elastic and strength analysis of CFRE composites for aerospace applications". *Aerosp. Sci. Technol.*, Vol. 60, pp. 96–107.

Koord, J., Stuven, J.L., Petersen, E., Volkerink, O. and Huhne, C., 2020. "Investigation of exact analytical solutions for circular notched composite laminates under tensile loading". *Compos. Struct.*, Vol. 243, No. 112180, p. 112180.

Mingming, G., Xiaoquan, C. and Qian, Z., 2017. "Compressive test and numerical simulation of center-notched composite laminates with different crack configurations". Polym. Compos., Vol. 38, No. 12, pp. 2631–2641.

Mollenhauer, D., Iarve, E.V., Kim, R. and Langley, B., 2006. "Examination of ply cracking in composite laminates with open holes: A moire interferometric and numerical study". *Compos. Part A Appl. Sci. Manuf.*, Vol. 37, No. 2, pp. 282–294.

Morais, A.B., 2000. "Open-hole tensile strength of quasi-isotropic laminates". *Compos. Sci. Technol.*, Vol. 60, No. 10, pp. 1997–2004.

Norton, R.L., 2013. *Projeto de máquinas: uma abordagem integrada*. Bookman Editora, Proto Alegre, Brazil, 4th edition.

Pierron, F., Green, B., Wisnom, M.R. and Hallett, S.R., 2007. "Full-field assessment of the damage process of laminated composite open-hole tensile specimens. part II: Experimental results". *Compos. Part A Appl. Sci. Manuf.*, Vol. 38, No. 11, pp. 2321–2332.

Pilkey, W.D. and Pilkey, D.F., 2008. *Peterson's Stress Concentration Factors*. John Wiley & Sons, Chichester, England, 3rd edition.

Saleh, M.N., Yudhanto, A., Potluri, P., Lubineau, G. and Soutis, C., 2016. "Characterising the loading direction sensitivity of 3D woven composites: Effect of z-binder architecture". *Compos. Part A Appl. Sci. Manuf.*, Vol. 90, pp. 577–588.

Shafighfard, T., Demir, E. and Yildiz, M., 2019. "Design of fiber-reinforced variable-stiffness composites for different open-hole geometries with fiber continuity and curvature constraints". *Compos. Struct.*, Vol. 226, No. 111280, p. 111280.

Sun, G., Wang, L., Chen, D. and Luo, Q., 2020. "Tensile performance of basalt fiber composites with open circular holes and straight notches". *Int. J. Mech. Sci.*, Vol. 176, No. 105517, p. 105517.

Tinô, S.R.L. and de Aquino, E.M.F., 2016. "Polymer composites: Effects of environmental aging and geometric discontinuity in the isotropic and anisotropic behaviors". *J. Compos. Mater.*, Vol. 50, No. 13, pp. 1771–1786.

Wang, J., Callus, P.J. and Bannister, M.K., 2004. "Experimental and numerical investigation of the tension and compression strength of un-notched and notched quasi-isotropic laminates". *Compos. Struct.*, Vol. 64, No. 3-4, pp. 297–306.

Warren, K.C., Lopez-Anido, R.A. and Goering, J., 2015. "Experimental investigation of three-dimensional woven composites". *Compos. Part A Appl. Sci. Manuf.*, Vol. 73, pp. 242–259.

Yudhanto, A., Watanabe, N., Iwahori, Y. and Hoshi, H., 2012. "The effects of stitch orientation on the tensile and open hole tension properties of carbon/epoxy plain weave laminates". *Mater. Eng.*, Vol. 35, pp. 563–571.

Zhu, F., Bai, P., Gong, Y., Lei, D. and He, X., 2018. "Accurate measurement of elastic modulus of specimen with initial bending using two-dimensional DIC and dual-reflector imaging technique". *Measurement (Lond.)*, Vol. 119, pp. 18–27.

6. RESPONSIBILITY NOTICE

The authors are the only responsible for the printed material included in this paper.